

# Modified Montmorillonite Clay Microparticles for Stable Oil-in-Seawater Emulsions

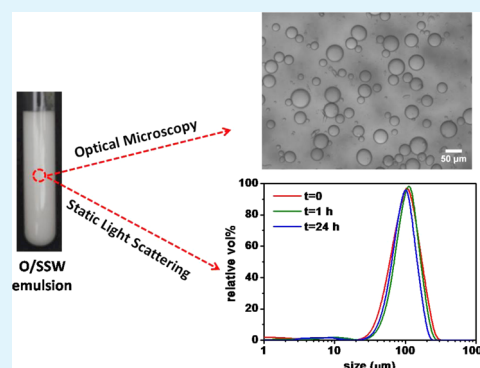
Jiannan Dong,<sup>†</sup> Andrew J. Worthen,<sup>†</sup> Lynn M. Foster,<sup>†,‡</sup> Yunshen Chen,<sup>†</sup> Kevin A. Cornell,<sup>†</sup> Steven L. Bryant,<sup>§</sup> Thomas M. Truskett,<sup>†</sup> Christopher W. Bielawski,<sup>‡</sup> and Keith P. Johnston<sup>\*,†</sup>

<sup>†</sup>McKetta Department of Chemical Engineering, <sup>‡</sup>Department of Chemistry and Biochemistry, and <sup>§</sup>Department of Petroleum and Geosystems Engineering, The University of Texas at Austin, Austin, Texas 78712-0231, United States

## S Supporting Information

**ABSTRACT:** Environmentally benign clay particles are of great interest for the stabilization of Pickering emulsions. Dodecane-in-synthetic seawater (SSW) emulsions formed with montmorillonite (MMT) clay microparticles modified with bis(2-hydroxyethyl)oleylamine were stable against coalescence, even at clay concentrations down to 0.1% w/v. Remarkably, as little as 0.001% w/v surfactant lowered the hydrophilicity of the clay to a sufficient level for stabilization of oil-in-SSW emulsions. The favorable effect of SSW on droplet size reduction and emulsion stability enhancement is hypothesized to be due to reduced electrostatic repulsion between adsorbed clay particles and a consequent increase in the continuous phase (an aqueous clay suspension) viscosity. Water/oil (W/O) emulsions were inverted to O/W either by decreasing the mass ratio of surfactant-to-clay (transitional inversion) or by increasing the water volume fraction (catastrophic inversion). For both types of emulsions, coalescence was minimal and the sedimentation or creaming was highly correlated with the droplet size. For catastrophic inversions, the droplet size of the emulsions was smaller in the case of the preferred curvature. Suspensions of concentrated clay in oil dispersions in the presence of surfactant were stable against settling. The mass transfer pathways during emulsification of oil containing the clay particles were analyzed on the droplet size/stability phase diagrams to provide insight for the design of dispersant systems for remediating surface and subsurface oceanic oil spills.

**KEYWORDS:** montmorillonite, clay, surfactant, emulsion, phase inversion, oil spills



## 1. INTRODUCTION

Natural clays, such as montmorillonite (MMT) and kaolinite, are known to disperse oil by forming oil mineral aggregates (OMAs). These aggregates are beneficial for dispersing oil spilled on beaches and in oceans<sup>1</sup> and form naturally as clay particles adsorb hydrophobic compounds, such as organic cations present in crude oil. As these compounds lower the hydrophilic–lipophilic balance (HLB), the clay particles become more surface active at the oil–water interface. This facilitates dispersion of oil at the ocean surface under shear produced by waves.<sup>2,3</sup> Large OMAs where the typical particle/oil mass ratio is large (e.g., 1:6 to 5:1) are sufficiently dense whereby they may settle on the seabed.<sup>4</sup> Despite extensive studies of these aggregates, little attention has been given to stabilization of oil droplets in the form of stable oil-in-seawater Pickering emulsions where the clay/oil mass ratio is much smaller. If the HLB of clay particles is modified with an appropriately chosen surfactant, then the particles make it possible to disperse oil droplets with extremely low dispersant concentrations. In the case for the Deepwater Horizon spill, the dispersant/oil concentration was large, about 1:5.

In Pickering emulsions, solid amphiphilic particles adsorb strongly at the interface and provide a barrier against droplet coalescence.<sup>5,6</sup> The wettability of the particles, characterized by

the contact angle  $\theta$ , influences the emulsion curvature and stability.<sup>7</sup> A wide variety of particles have been utilized including silica,<sup>8–12</sup> carbon black,<sup>13–15</sup> iron oxide,<sup>16–19</sup> and natural materials such as clay. Clay particles offer several distinctive advantages as emulsifiers: (i) They are natural, environmentally benign, and may be cost-effective for large scale applications.<sup>20</sup> (ii) As a consequence of the plate-like geometry, smaller masses are required to effectively cover a droplet interface relative to spherical particles.<sup>21</sup> (iii) The clay surfaces may be modified readily with amphiphiles to manipulate the contact angle at the oil–water interface.<sup>22</sup> (iv) They often form three-dimensional viscous networks in water, which may enhance stabilization of emulsified oil droplets.<sup>23</sup>

Both nanosized and microsized clay particles have been used to stabilize emulsions. Whereas the average diameter is only 30 nm for synthetic Laponite, it is much larger, typically 0.1 to 2  $\mu\text{m}$  for natural MMT. Although Laponite and MMT have similar thickness and density for fully exfoliated single platelets, the BET surface area of solid Laponite powder is between 350 and 400  $\text{m}^2/\text{g}$ , but only 30 to 100  $\text{m}^2/\text{g}$  for MMT given much

Received: April 10, 2014

Accepted: June 16, 2014

Published: June 16, 2014

less exfoliation.<sup>24</sup> Thus, it is possible that a smaller amount of surfactant would be required to modify the lower surface area for the micron-sized MMT particles relative to Laponite nanoparticles when partial exfoliation<sup>25</sup> occurs in the presence of an aqueous phase.

Given that clay particles are negatively charged and thus highly hydrophilic, their surfaces are typically modified with cationic surfactants via ion exchange to lower the HLB and raise the interfacial activity. Various studies have demonstrated that natural MMT may be modified in situ with cetyltrimethylammonium bromide (CTAB),<sup>26,27</sup> polyethylenimine,<sup>28</sup> ethoxylated quaternary alkylamine,<sup>29</sup> or dodecyltrimethylammonium bromide (DTAB)<sup>30</sup> to stabilize oil/water (O/W) emulsions. Commercial organoclays (for example, MMT after cation-exchanged with quaternary alkylamine salts) have a contact angle greater than 90° and stabilize water/oil (W/O) emulsions.<sup>31,32</sup> Several studies showed that synthetic Laponite upon in situ cation exchange with protonated amines, such as octadecylamine,<sup>33</sup> poly(oxypropylene)diamines,<sup>34</sup> and short-chain aliphatic amines,<sup>35</sup> also stabilize O/W emulsions. In addition to cationic modifiers, nonionic surfactants including glycerol monostearate, alkyl polyglucoside, and Span 80, have also been utilized to modify MMT<sup>22,36</sup> and Laponite<sup>37</sup> clays to stabilize O/W emulsions. The adsorption of the surfactant is driven by ion–dipole interactions with exchangeable cations on the clay surface and hydrogen bonding with the oxygen or hydroxyl groups.<sup>23</sup>

The high effective ionic strength of seawater of ~700 mM makes the formation of emulsions with clay particles challenging. The substantial Debye screening of electrostatic interactions may produce excess aggregation of clay particles and also modify particle adsorption onto an oil–seawater interface. In contrast, high salinities may provide benefits. Paunov et al.<sup>38</sup> demonstrated with a thermodynamic model that the adsorption of charged particles at the oil–water interface increases with added salt upon reducing the energy penalty of accumulating charged particles at the interface. In addition, salt addition can also reduce the kinetic repulsive adsorption barrier between like-charged particles and oil droplets.<sup>39,40</sup>

The effect of salt on emulsion stabilization has been investigated experimentally for a variety of types of particles at an ionic strength well below that of seawater. Ashby et al.<sup>41</sup> found that stable emulsions formed when Laponite particles were flocculated in 100 mM NaCl solutions, whereas they were not formed for the case of pure water. Binks et al.<sup>9,11</sup> demonstrated that the stability of O/W emulsions against coalescence could be improved by slightly flocculating silica particles upon adding up to 0.1 mM CaCl<sub>2</sub> or 2–5 mM LiCl<sub>3</sub>. Lagaly et al.<sup>22</sup> showed that 10 mM NaCl or 1 mM CaCl<sub>2</sub> enhanced the stability of emulsions prepared with MMT and nonionic surfactants against coalescence. For the extreme ionic strengths in seawater with the high concentration of divalent ions, new concepts may be required for modifying the surface properties of clay particles to stabilize oil/SSW emulsions, while avoiding droplet coalescence.

Emulsions undergo phase inversion from W/O to O/W observed for either transitional or catastrophic inversion.<sup>42–44</sup> A transitional phase inversion is governed by a change in the curvature of the interface by modifying the HLB of a surfactant or particle by varying, for example, temperature, pH, and salinity. In contrast, “catastrophic phase inversion” is observed upon varying the water volume fraction  $\phi_w$ . For an intermediate  $\phi_w$ , the emulsion type is determined primarily by the bending

energy (preferred curvature). According to Bancroft’s rule, the phase favored by the amphiphile is the continuous phase.<sup>45</sup> However, for a very low value of  $\phi_w$ , the favorable entropy of dispersing water in oil will produce a W/O emulsion even if the HLB is high and the surfactant or particle favors water. These inversions have been investigated for functionalized silica,<sup>46–48</sup> titanium dioxide,<sup>49</sup> iron oxide,<sup>16</sup> and latexes.<sup>50</sup> For emulsions stabilized with a mixture of particle and surfactant, only transitional phase inversions were investigated for MMT combined with CTAB,<sup>27</sup> Laponite combined with Span 80,<sup>51,52</sup> layered double hydroxide (LDH) combined with sodium dodecyl sulfate (SDS),<sup>53</sup> calcium carbonate combined with fatty acids,<sup>54</sup> and silica combined with double chain cationic surfactants.<sup>55,56</sup> Relatively little is known about the interplay between transitional and catastrophic phase inversions for particle/surfactant systems, and how they influence emulsion properties and stabilities, even without salt present.

Herein, dodecane-in-seawater emulsions were stabilized with natural MMT clay microparticles upon increasing the hydrophobicity (contact angle) by adsorption of a dilute oil soluble surfactant, bis(2-hydroxyethyl)oleylamine (E-O/12). Given that neither the high HLB clay nor low HLB surfactant alone stabilized these emulsions, the clay and surfactant were found to act synergistically. It was also demonstrated that an oil phase containing amphiphiles may be dispersed into droplets even though neither the microsized clay nor the unprotonated surfactant were dispersible in synthetic seawater (pH 8.2) even at high shear. Remarkably, the emulsions were formed even with only 0.001% w/v surfactant, far below the values of 0.01 to 1% w/v commonly used in other studies.<sup>22,28–30,36,52</sup> The synergistic emulsion formation and stabilization was pronounced in SSW. The interfacial and emulsion properties were explained in terms of the thermodynamic driving force for particle adsorption onto the oil–water interface, the kinetic adsorption barrier, and the high viscosity of aqueous clay suspensions. Both droplet size and emulsion stability were investigated over a wide range of surfactant/clay mass ratios, which governs the emulsion curvature, either O/W or W/O, and water volume fraction. From these measurements, phase inversion formulation-composition maps were constructed to identify both transitional inversion (curvature change) and catastrophic inversion (change in water volume fraction). Although these inversions have received little, if any, attention for the case of seawater, they are of great practical importance. We demonstrate that the clay-based dispersant could be colloidally stable in an oil phase at a high concentration (20% w/v with a viscosity of 278 cP at a shear rate of 10 s<sup>-1</sup>) and then sheared to disperse the oil in seawater. Collectively, these properties reflect the possibility of high storage stability, which is desirable for a broad range of practical applications, including oil spill remediation.

## 2. EXPERIMENTAL SECTION

**2.1. Materials.** Natural MMT (VAN GEL ES) was received as fine powder from R.T. Vanderbilt Company. The cation exchange capacity (CEC) of VAN GEL ES was approximately 50 mequiv/100 g per information provided by the manufacturer. Bis(2-hydroxyethyl)oleylamine (Ethomeen O/12LC or E-O/12), CH<sub>3</sub>(CH<sub>2</sub>)<sub>7</sub>CH=CH(CH<sub>2</sub>)<sub>8</sub>N(CH<sub>2</sub>CH<sub>2</sub>OH)<sub>2</sub>, was a gift from AkzoNobel Company. Muscovite mica sheets were obtained from Electron Microscopy Sciences. Synthetic seawater (SSW) was purchased from Ricca Chemical Company and used as received (pH 8.2). Dodecane was obtained from Acros Organics Company and passed through a basic alumina column to remove polar impurities prior to use. Deionized

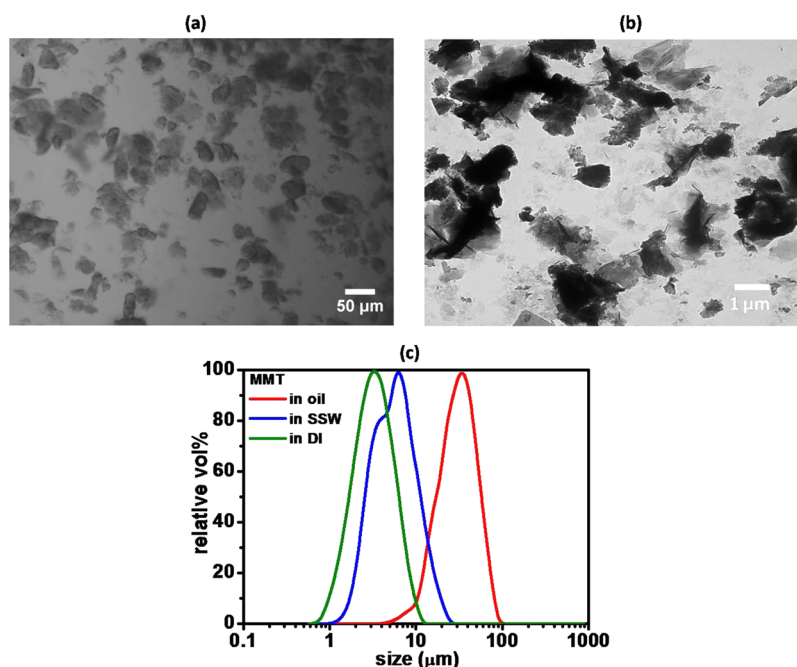


**Figure 1.** (a) Microscopic image of 1% w/v MMT particles in dodecane. (b) TEM image of MMT particles in DI water. (c) Typical size and size distribution of 1% w/v MMT particles in dodecane, SSW, and DI water, respectively, from static light scattering (Malvern Mastersizer). The experiments were also performed in dodecane, DI water, and SSW (not shown) with 0.001 wt % E-O/12 and the results were essentially identical to the distributions without surfactant.

(DI) water was prepared with a Nanopure II water purification system (Barnstead Company).

**2.2. Interfacial Tension Measurements.** The dodecane–SSW interfacial tension was measured using axisymmetric drop shape analysis of an aqueous pendant drop. The seawater drop was equilibrated for 5 min in dodecane, which contained a known concentration of surfactant and clay particles. For the dodecane samples containing surfactant and clay particles, they were allowed to equilibrate overnight in the dodecane without aqueous phase present before measurements. The drop shape profile was fitted to the Young–Laplace equation using a commercial package (CAM200, KSV Ltd., Finland). The reported mean value of the interfacial tension was an average of 10 measurements acquired every 10 s and the standard deviation was typically within 1% of the mean value.

**2.3. Contact Angle Measurements.** Mica was used as a model clay substrate. Although mica may not be a perfect match for MMT because of its higher surface charge density, it is similar in both composition and crystal structure to many clays<sup>35</sup> and can be easily cleaved to produce smooth and uniform surface for contact angle measurements. Freshly cleaved mica sheets were equilibrated overnight with surfactant at various concentrations in dodecane. A drop of  $\sim 10 \mu\text{L}$  SSW was placed on a mica surface and the drop shape profile was analyzed with a software package (CAM200, KSV Ltd., Finland) to obtain the contact angle.

**2.4. Preparation of Modified Clay Suspensions and Emulsions.** Oil-based clay suspensions were prepared by mixing MMT particles with E-O/12 surfactant in dodecane using an IKA Ultra-Turrax T-25 with an 8 mm head operating at 13 500 rpm for 10 min at room temperature. Emulsions were prepared by combining DI water or SSW and dodecane containing a given amount of surfactant-modified clay suspension to a total volume of 10 mL and emulsified with the same homogenizer operated at 13 500 rpm for 2 min at room temperature. Clay and surfactant concentrations are denoted as mass percent per total sample volume (% w/v) and water volume fraction  $\phi_w$  is given as the fraction of aqueous phase to the total sample volume. Immediately after emulsification, the emulsion type was determined from the conductivity measured with a Cole–Parmer EC conductivity meter equipped with a Pt/Pt black electrode. The emulsion type was also inferred by observing the outcome of a drop of

emulsion added to either pure oil or pure water. If a droplet of emulsion dispersed in water, it was aqueous continuous, and if it dispersed in oil, it was oil continuous.

**2.5. Characterization of Clay Particles.** BET surface analysis of clay powder was performed with nitrogen sorption using a Quantachrome Instruments NOVA 2000 high-speed surface area BET analyzer at a temperature of 77 K. Prior to measurements, the sample was degassed in vacuum for 3 days at room temperature. The specific surface area was determined in the relative pressure range ( $P/P_0$ ) of 0.05 to 0.40. Transmission electron microscopy (TEM) imaging was performed on a FEI TECNAI G2 F20 X-TWIN instrument. A drop of  $\sim 20 \mu\text{L}$  dilute aqueous dispersion of clay particles was deposited onto a 200 mesh carbon-coated copper TEM grid and air-dried prior imaging. Optical microscopy of clay particles was performed with a Nikon Eclipse ME600 light microscope fitted with a Photometrics digital camera. Clay size and size distribution in a medium (DI water, SSW or dodecane) were measured with a Malvern Mastersizer S static light scattering (SLS) instrument with a 15 mL stirred optical sample cell filled with the corresponding medium. Refractive indices of 1.33, 1.42, and 1.52 were used for aqueous phase (DI and SSW), dodecane, and MMT, respectively.

**2.6. Characterization of Emulsion Properties.** Freshly prepared emulsions were transferred to capped glass test tubes with a diameter of 16 mm and a length of 125 mm. The emulsion stability to the gravity-induced phase separation was assessed by monitoring the creaming front position for O/W emulsions or the sedimentation front for W/O emulsions as a function of time using a Nikon DS100 camera with a Phottix TR-90 time controller. The digital photos were analyzed with ImageJ software (US National Institutes of Health). The emulsion stability was quantified as the time required to resolve 20% of the initial volume of the continuous phase. Emulsion droplet size distributions were measured using a Malvern Mastersizer S with a 15 mL stirred optical sample cell. Approximately  $20 \mu\text{L}$  of emulsion was added to the sample cell filled with SSW (for O/W) or dodecane (for W/O). Optical microscopy of emulsions was performed with a Nikon Eclipse ME600 light microscope fitted with a Photometrics digital camera.



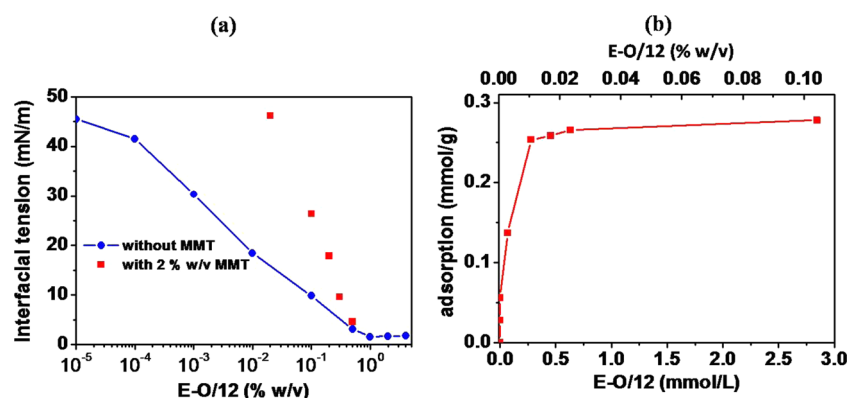


**Figure 2.** (a) Dodecane/synthetic seawater interfacial tension of E-O/12 with and without 2% w/v MMT. (b) Adsorption isotherm of E-O/12 on MMT particles determined from data in panel a by material balance. Note that the surfactant and MMT were equilibrated in the dodecane phase without aqueous phase present.

### 3. RESULTS AND DISCUSSION

**3.1. Properties of Clay Particles.** The BET surface area of as received MMT powder was measured to be 51.5 m<sup>2</sup>/g. As shown by optical microscopy in Figure 1a, the size of MMT particles in dodecane was quite large, 10–50  $\mu$ m. Upon hydration in DI water, the TEM image in Figure 1b showed that the MMT partially exfoliated to form small stacks of platelets with a particle size between 1 and 5  $\mu$ m. The static light scattering measurements (Figure 1c) showed that the average clay size was 3, 6, and 30  $\mu$ m in DI water, SSW, and dodecane, respectively. Again, the clay underwent exfoliation in the aqueous media. In each case, the polydispersity was relatively large. The particle size was larger in SSW than that in DI water, resulting from substantial particle aggregation by significant electrostatic charge screening.

**3.2. Effect of Surface Modification of Clay Particles on Interfacial Properties and Partition Behaviors.** The dodecane/SSW interfacial tension ( $\gamma$ ) was reduced by the addition of E-O/12 in dodecane up to ~1% w/v E-O/12. At higher concentrations,  $\gamma$  did not decrease further (Figure 2a), indicating a critical reverse micelle concentration of E-O/12 in dodecane of ~1% w/v. As a control, the dodecane/SSW interfacial tension was measured without addition of surfactant in the absence and presence of clay particles. It did not change with the addition of bare clay particles, suggesting that surface-active contaminants were not present. At a given surfactant concentration, the interfacial tension increased when clay particles were added. This difference was due to the adsorption of surfactant on the particle surface, leaving less free surfactant available for adsorption at the oil/SSW interface (Figure 2a).

To quantify the extent of surfactant adsorption on clay particles in oil, the adsorption isotherm was determined by a material balance by quantifying the free surfactant concentration from the measured interfacial tension.<sup>8,57</sup> As shown in Figure 2b, the adsorption increased rapidly with surfactant concentration and then reached a plateau. The suspension pH was 8.2 with only MMT present and was found to be nearly constant with addition of E-O/12, where 0.1% w/v E-O/12 increased the pH to 8.4. The maximum adsorption was found to be about 0.28 mmol/g, which was much smaller than the values from 0.7 to 1.3 mmol/g for other alkyl ammonium salts on MMT particles.<sup>58</sup> For a measured BET surface area of 51.5 m<sup>2</sup>/g, the upper bound on the adsorption density was 5.4  $\mu$ mol/m<sup>2</sup> with an area per surfactant of 30  $\text{Å}^2$ . However, the area per surfactant will be considerably larger than this value, as

the MMT undergoes significant exfoliation in the presence of water (Figure 1).

The wettability alteration of MMT surfaces by adsorption of surfactant was evaluated by contact angle measurements using mica as a surrogate material. The contact angle of a SSW drop on a mica sheet was plotted as a function of the surfactant concentration in the oil phase (Figure 3). The contact angle in

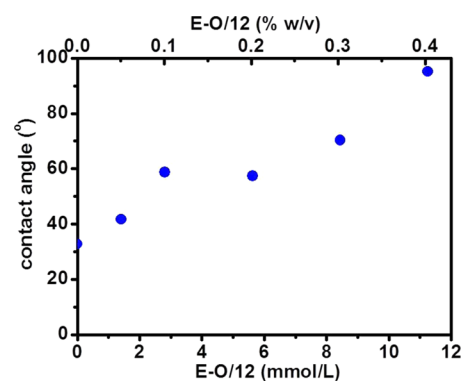


**Figure 3.** Contact angle of synthetic seawater drop on mica (used as a surrogate for MMT) in the presence of dodecane as a function of E-O/12 concentration.

the absence of surfactant was 33°, which is similar to the value of 31° for a DI water drop on a mica sheet in liquid paraffin.<sup>35</sup> With increasing surfactant concentration, the contact angle increased and reached to 95° at 0.4% w/v E-O/12. This increase in hydrophobicity results from the surfactant tails extending into the oil phase, whereas the two ethylene oxide (EO) groups and the amine in the headgroup interact with the clay dipoles and charged sites, as has been observed for other nonionic surfactants.<sup>23</sup> Here E-O/12 is essentially unprotonated in SSW at pH 8.2 (see Supporting Information Figure S1).

The partitioning behavior of the clay particles with different surface modification extents were compared with that of unmodified clay particles (Figure 4). One milliliter of dodecane containing clay particles was applied onto the top of 1 mL of SSW under quiescent conditions. The unmodified clay particles settled from the oil due to gravity and then entered the aqueous phase. At low mass ratios of surfactant to clay (e.g., 0.02), a significantly smaller amount of particles entered the aqueous phase. At high mass ratios of surfactant to clay (e.g., 0.1 or 0.2),

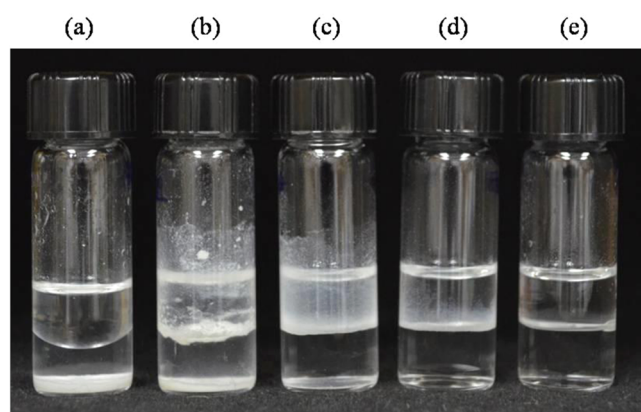


**Figure 4.** Partitioning behavior of unmodified and modified MMT clay particles after 1 week. The clay concentration in all samples was kept at 0.5% w/v with respect to the total volume of dodecane and synthetic seawater. The mass ratios of surfactant to clay in (a) to (e) were 0, 0.02, 0.05, 0.1, and 0.2, respectively. Clay was observed in the bottom of the aqueous phase in panels a and b, but not in the aqueous phase in panels d and e as the modified clay became more hydrophobic.

nearly all modified clay particles were trapped at the oil/water interface and the particles did not enter the aqueous phase. Similarly, Binks et al.<sup>32</sup> observed that commercial organoclay particles initially introduced in isopropyl myristate (IPM) sedimented down to the IPM–water interface. The drastic difference in the partitioning behavior between the unmodified and modified clay particles was consistent with the surface hydrophilicity/hydrophobicity determined from the contact angle. From the point of view of practical dispersants for oil in water, the small loss of particles to the aqueous phase as a consequence of the low hydrophilicity surfaces would be highly beneficial.

### 3.3. Effect of Surfactant Modification of Clay and Salinity on Emulsion Properties.

In a control experiment without any added surfactant, MMT clay particles were too hydrophilic to stabilize emulsions. Similarly, emulsions formed with E-O/12 surfactant alone with a concentration below 0.1% w/v in the unprotonated state were very unstable and resolved within seconds either with or without added salt. Here the HLB was too low for an unprotonated amine with only two ethoxy groups. For example, the partition coefficient for E-O/12 was estimated to be on the order of  $10^7$  from the measured partition coefficients of a series of ethoxylated alkylamines with two EO groups between heptane and alkaline water.<sup>59</sup> However, the combination of MMT and E-O/12 will be shown to be synergistic for formation of stable emulsions with relatively small amphiphile concentrations.

Macroscopic and microscopic observations of the emulsions formed in DI water and SSW are shown in Figure 5. With the same clay and surfactant concentration, the emulsion creamed much more slowly with added salt as shown in the photograph of the test tubes. When DI water was changed to SSW, the viscosity of the continuous phase increased from 1.3 to 8.5 cP, improving creaming stability. For the SSW case, the creamed aqueous phase was clear, indicating that most clay particles were incorporated in the emulsion phase. In contrast, the creamed aqueous phase in the DI water case was turbid, which suggests that many clay particles were released from the emulsion phase. The optical microscopic images also showed that the spherical oil droplets in the SSW case were much smaller. The time-dependent droplet size distributions of the DI water and SSW cases are compared in Figures 5c and 5d. The initial droplet size decreased from 180 to 86  $\mu\text{m}$  when the continuous aqueous phase was changed from DI water to SSW. The droplet size in the DI water case increased over time while the droplet size in the SSW case remained almost the same even after 1 day. Collectively, the emulsions formed in SSW

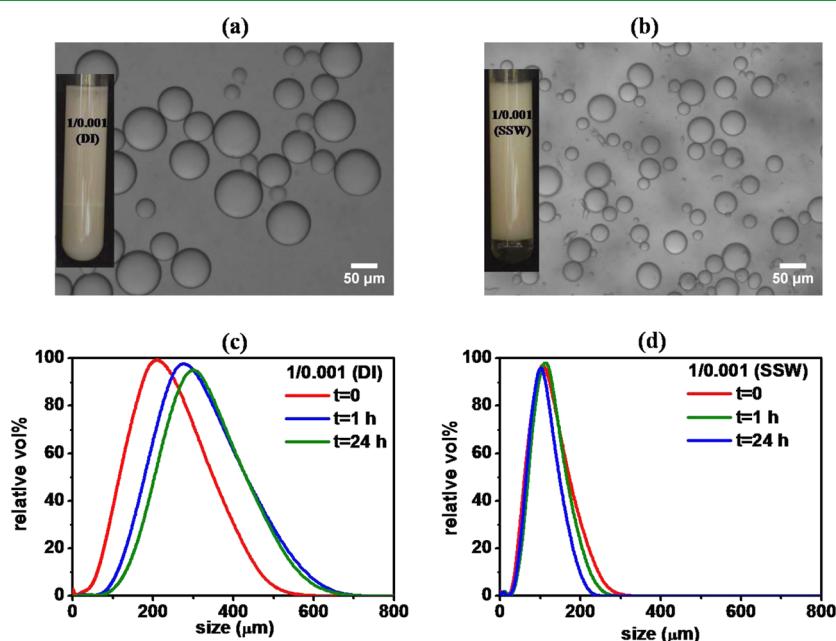


**Figure 5.** Photographs of emulsion resolution after 1 h (insets in panels a and b) and optical microscopy images of a dodecane-in-DI water emulsion in panel a and a dodecane-in-synthetic seawater emulsion in panel b, and the corresponding time-dependent droplet size distributions for the dodecane-in-DI water emulsion in panel c and for the dodecane-in-synthetic seawater emulsion in panel d. The emulsions were prepared with 1% w/v MMT and 0.001% w/v E-O/12 (1/0.001) at a water volume fraction of 0.5.

were composed of smaller droplets and were more stable to coalescence and creaming.

As shown in Figure 6, the droplet size in the DI water case decreased from 180 to 75  $\mu\text{m}$  when the surfactant

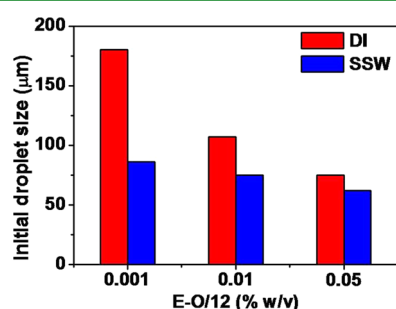


**Figure 6.** Initial droplet size of O/W emulsions with 1% w/v MMT and three E-O/12 concentrations, formed with DI water (red) or synthetic seawater (blue). The water volume fraction was 0.5.

concentration increased from 0.001 to 0.05% w/v, given the ability of shear to overcome the Laplace pressure for the lower  $\gamma$ . Additionally, the modified clay particles became more hydrophobic at higher surfactant concentrations, favoring adsorption onto the oil–water interface for stabilization against coalescence of initially formed oil drops. For the same increase in surfactant concentration, the initial droplet size in the SSW decreased only slightly from 86 to 62  $\mu\text{m}$ . Remarkably, the droplet size was only 86  $\mu\text{m}$  for an extremely low E-O/12 concentration of 0.001% w/v. The high salinity facilitated initial formation of small droplets during emulsification process by driving the clay particles from the brine phase to the oil/water interface. This salt effect was less pronounced at a high surfactant concentration (e.g., 0.05% w/v), where the dominant effect was that of surfactant on lowering  $\gamma$ . A secondary effect is greater wettability alteration of the clay with the increase in surfactant concentration, which drives the clay particles to the interface.

As shown in Figure 7a, the combination of clay with a concentration ranging from 0.1 to 1% w/v and surfactant with a concentration from 0.001 to 0.1% w/v led to a strong

synergistic stabilization for dodecane-in-SSW emulsions at a water volume fraction of 0.5. For all of the cases presented in Figure 7, the emulsion type was O/W and no phase inversions were observed. The phase inversions induced by further increasing surfactant-to-clay ratio or varying water volume fraction will be presented in Figure 9 and discussed in Section 3.5. These emulsions were quite stable to coalescence since the average droplet size and size distribution changed little over time (Supporting Information Figure S2). No coalescence was observed even at the lowest MMT concentration of 0.1% w/v. The largest initial droplet size was above 200  $\mu\text{m}$  at low amphiphile concentrations. Only a very small surfactant concentration was required relative to the clay concentration for all the cases. For the lower clay concentrations, the droplet size decreased down to 100  $\mu\text{m}$  as the surfactant concentration increased, presumably because of a reduction in interfacial tension, as well as modification of the clay surface. However, as the clay concentration increased to  $\sim 0.8\%$  w/v, 50  $\mu\text{m}$  droplets were formed even at the lowest surfactant concentration. Without surfactant, the droplets were however on the order of millimeters in diameter, consistent with the little reduction in the interfacial tension (small surface pressure). Without clay, the surfactant at 0.001% w/v did not produce emulsions. Thus, we attribute the synergistic effect of the extremely low surfactant concentration of 0.001% w/v in either DI water (Figure 5c) or SSW (Figures 5d and 7a) to modification of the clay by the surfactant, which may influence exfoliation and interfacial activity. Furthermore, this effect was even stronger for SSW as the salt drove the clay toward the interface. When a sufficient amount of clay ( $>0.8\%$  w/v) was added, only a very small amount of surfactant (as low as 0.001% w/v) is required to obtain O/W droplets below 70  $\mu\text{m}$ , which is the desired oil droplet size for biodegradation by bacteria in the ocean.<sup>14</sup>

The resolution of the emulsions was primarily because of creaming, given the aforementioned small amount of coalescence, as shown in Figure 7b. The contours were relatively vertical suggesting the emulsion stability was influenced primarily by the clay concentration, and relatively little by the surfactant. As the MMT concentration increased from 0.1% to 0.5% and to 1% w/v, the viscosity of the

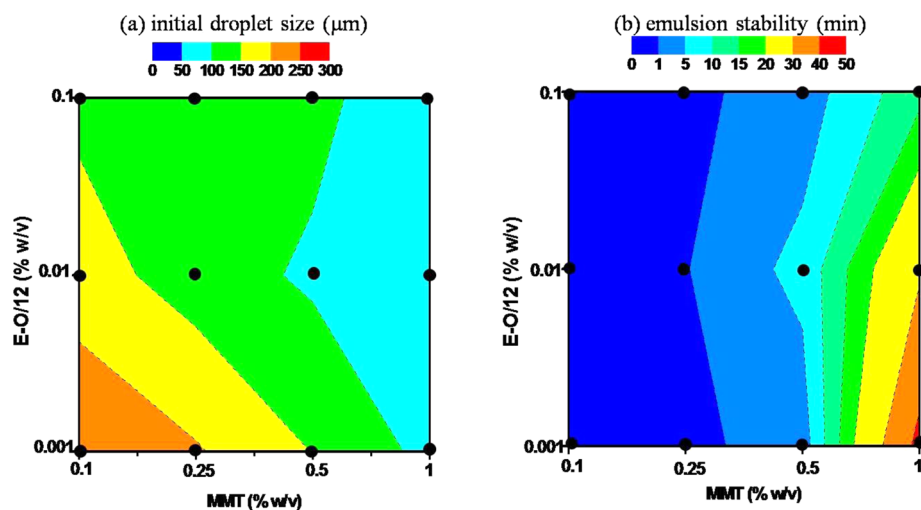


**Figure 7.** Contour maps of initial droplet size (a) and emulsion stability (time to resolve 20% of the continuous phase) (b) for dodecane-in-synthetic seawater emulsions prepared with various concentrations of MMT and E-O/12 at a water volume fraction of 0.5. The black dots represent O/W emulsions.

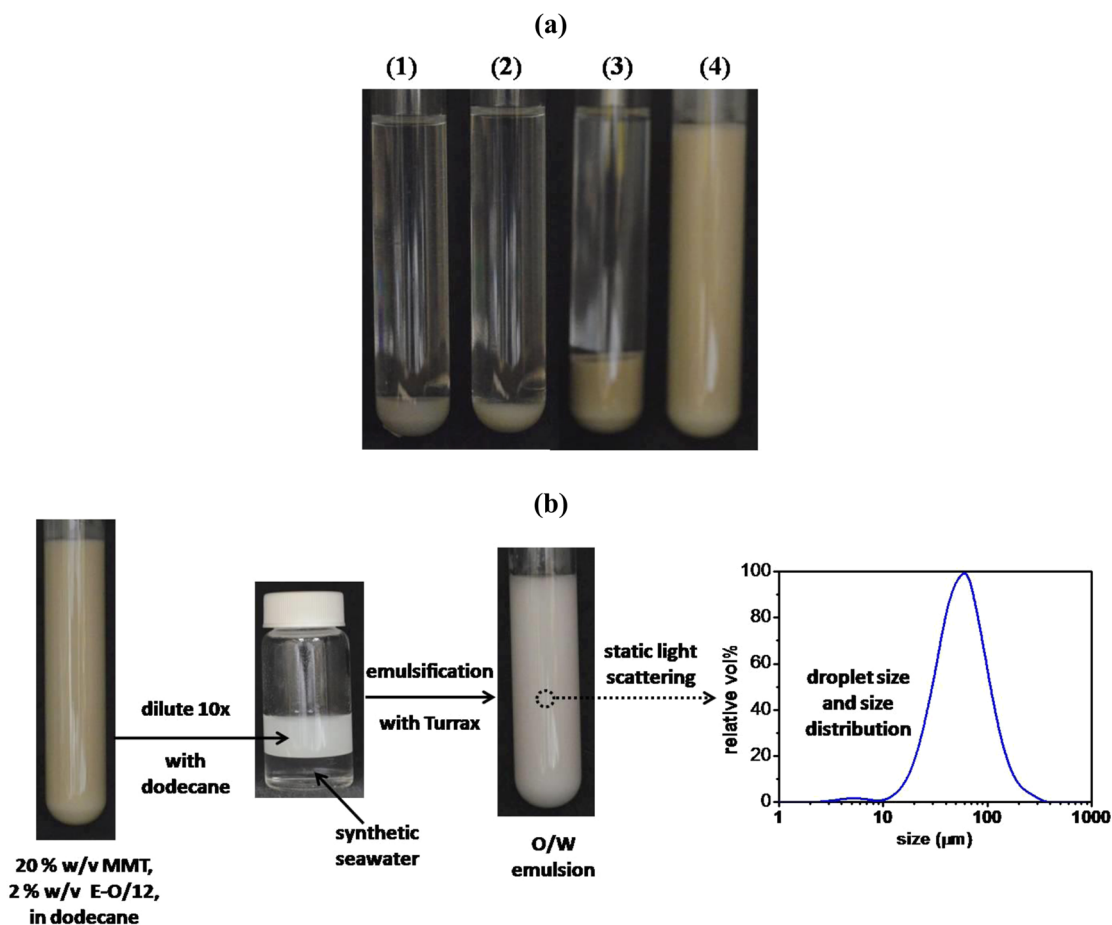


**Figure 8.** (a) Settling behavior of unmodified and modified MMT clay particles in dodecane after 1 day: (1) 1% w/v MMT, (2) 1% w/v MMT modified with 0.1% w/v E-O/12, (3) 20% w/v MMT, and (4) 20% w/v MMT modified with 2% w/v E-O/12. (b) Schematic of diluting a 20% w/v MMT modified with 2% w/v E-O/12 in dodecane by 10-fold to a final concentration of 1% w/v MMT and 0.1% w/v E-O/12 and shearing with SSW at a water volume fraction of 0.5.

continuous phase increased from 1.2, to 2.7, and to 8.5 cP (see Supporting Information). Accordingly, the creaming rate would be reduced given that creaming rate is inversely proportional to the viscosity. In addition, the reduction in the droplet size with the increasing MMT concentration could also decrease the creaming rate, which is proportional to the square of the droplet size. A theoretical creaming rate can be calculated from the Stokes' law which balances buoyancy against viscous drag of a spherical droplet in a dilute system. When the hindered effect on the creaming rate due to a substantial dispersed phase volume is considered, the empirical Richardson–Zaki<sup>60</sup> equation can be used to estimate a corrected creaming rate. For nearly all the cases, the experimental stability was found to be between the stability from the Stokes' law and that from the Richardson–Zaki model (Supporting Information Table S1). Other factors such as droplet size polydispersity and interdroplet attraction may also need to be taken into account for a better prediction of the creaming stability.

The high salinity in SSW raises the thermodynamic driving force for clay particle adsorption at the O/W interface by reducing the energy penalty of concentrating the charged particles at the interface.<sup>38</sup> The work  $W_{el}$  required to bring charged particles to the interface is given by<sup>38</sup>

$$W_{el} \approx \frac{A}{2\epsilon_0\epsilon_r\kappa} (\sigma_{ow,f}^2 - \sigma_{ow,i}^2) \quad (1)$$

where  $A$  is the area of the oil–water interface,  $\epsilon_0$  is the dielectric constant of vacuum,  $\epsilon_r$  is the relative dielectric constant of the electrolyte solution,  $\kappa$  is the Debye screening parameter,  $\sigma_{ow,f}$  is the effective charge density of the interface after particle adsorption, and  $\sigma_{ow,i}$  is the initial charge density of the interface before particle adsorption. Thus, the barrier  $W_{el}$  is proportional to the Debye length  $\kappa^{-1}$ , which decreases with the square root of the ionic strength.

Emulsion formation relies on overcoming the barrier for adsorption of the particles at the oil–water interface on the basis of DLVO theory. The adsorption of particles onto the droplet interface is governed by the balance between the hydrodynamic force pushing the particles toward the droplet surface and the repulsive electrostatic force hindering the adsorption of particles. For turbulent flow in a rotor–stator mixer for emulsification, the hydrodynamic driving force  $F_{mix}$  between a particle and an oil droplet can be estimated from the expression,<sup>61</sup>

$$F_{mix} \approx a^2 \rho_c \epsilon^{2/3} R^{2/3} \quad (2)$$

where  $a$  is the particle radius,  $R$  is the oil droplet radius,  $\rho_c$  is the continuous phase density, and  $\epsilon$  is the rate of energy dissipation per unit mass. The adsorption of the negatively charged clay particles onto negatively charged oil droplet interfaces, due to spontaneous and preferential adsorption of hydroxyl ions,<sup>62</sup> must overcome the electrostatic repulsion. The



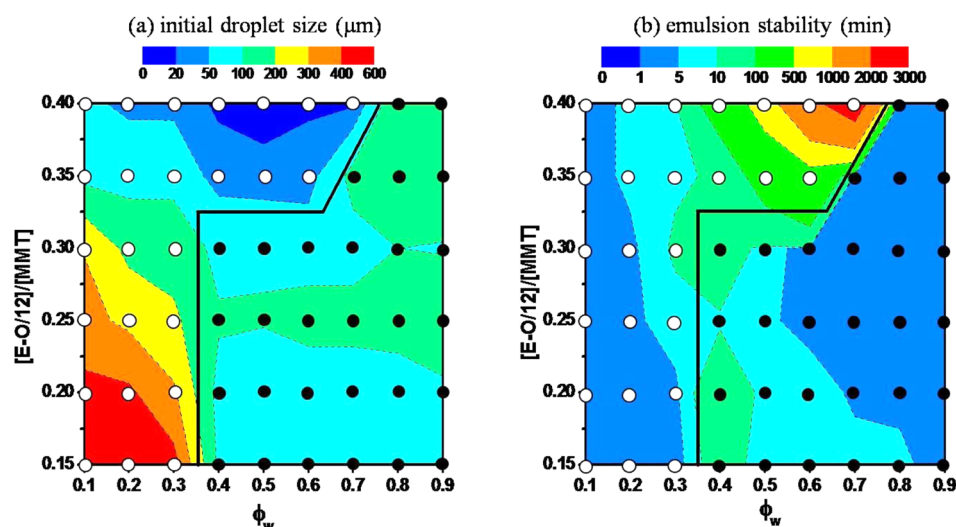


**Figure 9.** Contour maps of (a) initial droplet size and (b) emulsion stability (for resolution of 20% of the continuous phase) as a function of the mass ratio of surfactant-to-clay and water volume fraction at a fixed total concentration of surfactant and clay of 1.1% w/v. The black dots represent O/W emulsions and the white dots represent W/O emulsions. The bold black solid line represents the boundary between O/W and W/O emulsions.

high ionic strength of SSW leads to substantial electrostatic charge screening such that the kinetic repulsion barrier between clay particles and oil droplets becomes negligible, thereby promoting the approach of clay particles to newly formed bare oil drops during emulsification, as observed recently for a related system.<sup>12</sup> Furthermore, the average size of clay particles increased from 3  $\mu\text{m}$  in DI water to 6  $\mu\text{m}$  in SSW (Figure 1), which increases  $F_{\text{mix}}$ . Similarly, Golemanov et al.<sup>39</sup> reported that the formation of stable W/O emulsions with charged latex particles required a relatively high concentration of electrolyte in the aqueous phase to lower the electrostatic barrier to particle adsorption at the oil/water interface.

The plate-like structure of MMT is highly efficient for stabilizing oil–water interfaces with minimal mass of material<sup>21</sup> in contrast to spherical particles with a relatively greater amount of mass in the normal direction to the interface. For spheres, the maximum capillary pressure  $P_c^{\text{max}}$  responsible for stability against droplet coalescence is inversely proportional to the sphere radius  $a_s$ , that is  $P_c^{\text{max}} \propto 1/a_s$ .<sup>63</sup> However, the adsorption energy  $\Delta E$ , which is the energy required to remove a sphere from the oil–water interface, is proportional to  $a_s^2$ , that is  $\Delta E \propto a_s^2$ . Here, the maximum capillary pressure requires a small radius while a strong adsorption energy requires a large radius. For plate-like particles with two length scales, thickness  $h$  and lateral size  $2a_d$ , the aforementioned dichotomy for spheres may be overcome. Here, thickness  $h$  could serve as a reasonable proxy for sphere diameter in the role of preventing droplet coalescence. The maximum capillary pressure is therefore given by  $P_c^{\text{max}} \propto 1/h$ . The plate lateral size primarily determines the adsorption energy, which is expressed as  $\Delta E \propto a_d^2$ . Consequently, plate-like particles with high aspect ratios ( $2a_d/h$ ) are more effective emulsion stabilizers<sup>64</sup> than spheres for a given mass. In essence, a smaller mass blocks a larger fraction of the interface.

In summary, when MMT particles are combined with E-O/12 surfactant, as low as 0.001% w/v of surfactant corresponding to only a small fraction of the mass of clay, was required to achieve the desired wettability of the clay particles for the oil–water interface. The presence of seawater further promotes the emulsification efficiency and stabilization effectiveness, owing to

a combined effect of a smaller electrostatic kinetic adsorption barrier, an enhanced viscosity of the continuous phase, and an increased thermodynamic driving force for particle adsorption. Whereas a model oil dodecane was utilized in this study, ionic compounds in crude oil such as anionic naphthenic acids may influence the surface of the clay particles, but likely to a lesser extent than cations.

### 3.4. Nonsettling Concentrated Clay Dispersions in Oil.

Although the dilute MMT-based dispersant system (1% w/v) successfully emulsified and stabilized the oil droplets, the initial dispersions of large clay particles (not exfoliated in oil) and surfactant in the oil were not colloiddally stable and settled within minutes. For practical applications, such as dispersants for oil leaks, it would be desirable to have high storage stability in a lipophilic phase that can wet oil. It is shown in Figure 8a that the surfactant modified MMT clay particles become stable against settling at a high clay concentration with the mass ratio of surfactant-to-clay fixed. Unmodified MMT particles settled within seconds regardless of particle concentration (Figures 8a1 and 8a3). After modification with surfactant to enhance wetting of clay by oil, 1% w/v MMT clay particles with 0.1% w/v E-O/12 settled within minutes (Figure 8a2) while 20% w/v MMT clay particles with 2% w/v E-O/12 exhibited negligible settling over at least 1 day (Figure 8a4). The viscosity of this concentrated clay-based dispersant was found to be 278 cP at a shear rate of 10  $\text{s}^{-1}$ . The settling of clay particles was dramatically hindered due to the increased particle volume fraction whereby the clay particles formed a viscous gel.

A typical example of using such a concentrated clay dispersant for the formation and stabilization of dodecane-in-SSW emulsions is given in Figure 8b. Upon dilution and emulsification which mimics the delivery and application of dispersant for treating oil spills, the resulting clay-based dispersant produced an O/W emulsion with an average droplet size of 60  $\mu\text{m}$  and a creaming stability of 20 min at a water volume fraction of 0.5. For the same final concentrations of clay and surfactant, an initially dilute dispersant formed an O/W emulsion with an average droplet size of 64  $\mu\text{m}$  and a creaming stability of 15 min at the same water volume fraction. Thus, the dilution process does not change the dispersant performance.



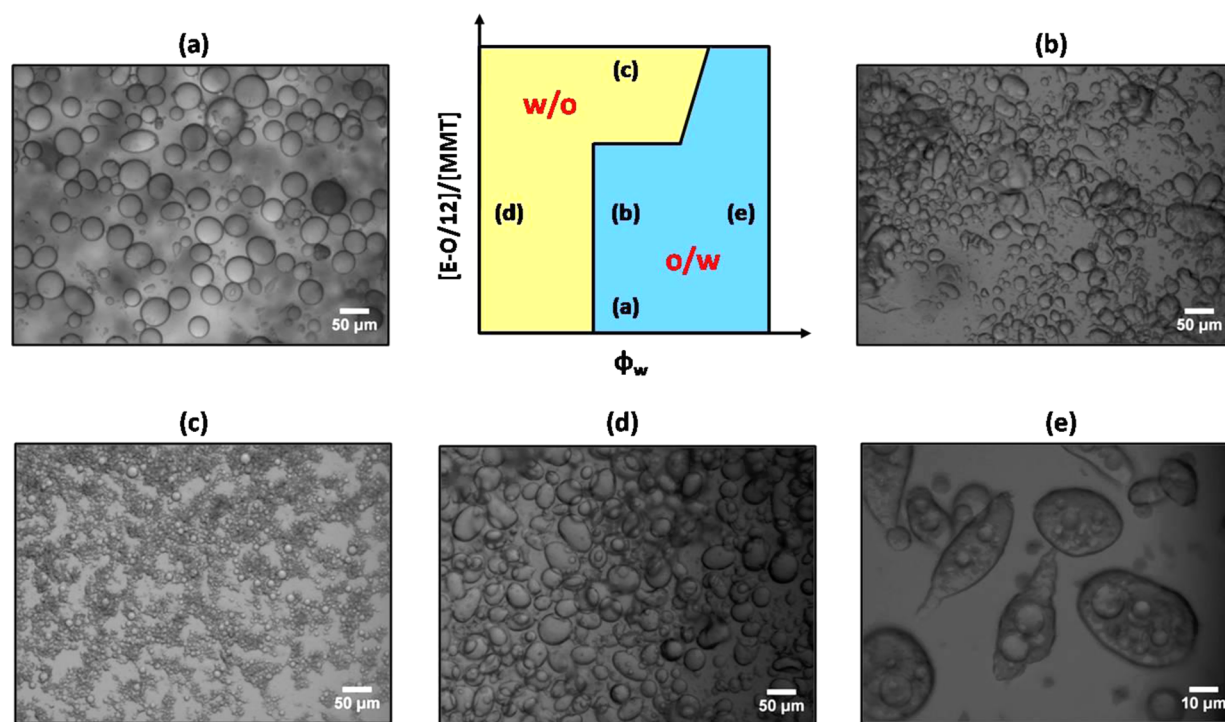


**Figure 10.** Optical microscopic pictures of the emulsions prepared at various combinations of mass ratio of surfactant to clay and water volume fraction: (a) spherical O/W droplets, (b) elongated O/W droplets, (c) small W/O droplets, (d) large W/O droplets, and (e) w/O/W droplets. The total concentration of clay and surfactant was fixed at 1.1% w/v.

**3.5. Phase Inversions and Associated Emulsion Properties.** The global behavior of the role of the mass ratio of surfactant-to-clay (HLB formulation variable) and the water volume fraction on emulsion type, droplet size, and stability may be best understood on a phase diagram. As has been shown for surfactant-stabilized emulsions,<sup>44</sup> a formulation-composition bidimensional map (Figure 9) was constructed at a fixed total concentration of MMT and E-O/12 of 1.1% w/v. All of the detailed data used to construct the map are shown in Supporting Information Table S2. The bold black solid line represents the boundary between O/W and W/O emulsions. The emulsion type was inverted from O/W to W/O either by increasing the mass ratio of surfactant-to-clay (transitional inversion) in a particular range of  $\phi_w$  or by decreasing  $\phi_w$  (catastrophic inversion). Both O/W and W/O emulsions were quite stable against coalescence given that the droplet size and size distribution varied little over time (see Supporting Information Figure S3). The primary emulsion destabilization mechanism is therefore gravity induced phase separation, that is creaming for O/W emulsions and sedimentation for W/O emulsions, as quantified in Figure 9b. The emulsion stability will be shown to be correlated with the droplet size.

We begin by considering changes in  $[E-O/12]/[MMT]$  for a fixed  $\phi_w$  to examine the transitional inversion in curvature. For all of the results to this point,  $\phi_w$  was 0.5 and the  $[E-O/12]/[MMT]$  ratios were low such that the HLB was high and only O/W emulsions were present. In Figure 9, the  $[E-O/12]/[MMT]$  ratio was increased to invert the curvature to a W/O emulsion for a range of  $\phi_w$ . At an immediate  $\phi_w$  (e.g., 0.5), the O/W droplet size was moderately large between 50 and 200  $\mu\text{m}$  for a  $[E-O/12]/[MMT]$  ratio smaller than 0.35. Accordingly, the emulsion stability was between 10 and 100 min. For the highest  $[E-O/12]/[MMT]$  ratio, a W/O emulsion was formed with a very small droplet size ( $<20 \mu\text{m}$ ), along with

a higher emulsion stability of around 1000 min. The smaller W/O droplet size is mainly due to the presence of larger amount of surfactant available for reducing the interfacial tension. Interestingly, the stability did not become low at the transitional inversion as it does for surfactant stabilized emulsions<sup>65</sup> where it is easy to generate channels for coalescence by changes in curvature with the small bending moment.<sup>66</sup> For the adsorbed particles, it appears that the interface is more rigid and these channels do not form. At a high  $\phi_w$  ( $>0.7$ ), the stability of the corresponding O/W emulsions was poor ( $\sim 1$  min), independent of the  $[E-O/12]/[MMT]$  ratio. Similarly at a low  $\phi_w$  ( $<0.3$ ), the corresponding W/O emulsions exhibited very low stability because of large droplet size.

We now consider changes in  $\phi_w$  at a fixed  $[E-O/12]/[MMT]$  ratio to examine catastrophic phase inversions. For a  $[E-O/12]/[MMT]$  ratio below 0.35 (e.g., 0.15), the emulsion morphology inverted from O/W to W/O at a catastrophic inversion point of  $\phi_w \approx 0.35$ . For the O/W emulsions, Bancroft's rule was observed and the droplet size was between 50 and 100  $\mu\text{m}$ . On the left side, where the curvature was the opposite of the preferred curvature, the droplet size was much larger ( $\sim 400 \mu\text{m}$ ). The preferred curvature is the curvature favored by the contact angle of the amphiphiles at the interface independently of any influence on the curvature from droplet interactions which are influenced by the oil/water ratio. For example, the curvature is the opposite of the preferred curvature in the bottom-left and top-right corners of the phase diagram. The preferred curvature is often measured at equal volumes of oil and water. Similarly for a  $[E-O/12]/[MMT]$  ratio above 0.35 (e.g., 0.4), the preferred curvature was W/O emulsions according to Bancroft's rule and the droplet size was small ( $\sim 20 \mu\text{m}$ ). Correspondingly, the O/W emulsions on the right side of the inversion boundary, where

the curvature was opposite of the preferred curvature consisted of large droplets ( $\sim 200 \mu\text{m}$ ). The smaller droplet size for the preferred emulsion type has also been reported by Binks et al.<sup>46,48</sup> using silica particles and by Stiller et al.<sup>49</sup> using  $\text{TiO}_2$  particles. As the  $[\text{E-O}/12]/[\text{MMT}]$  ratio increased from 0.2 to 0.35 and to 0.4, the value of  $\phi_w$  where catastrophic inversion occurred increased from 0.35 to 0.65 and to 0.75. Thus, the required  $\phi_w$  for catastrophic inversion increased with the hydrophobicity of modified clay particles. This trend is in good agreement with Kaptay's prediction that the water volume fraction where catastrophic inversion occurred increased with the contact angle of solid particles.<sup>67</sup>

Optical micrographs of the emulsion droplet morphology are also shown for various surfactant-to-clay ratios and water volume fractions in Figure 10. The sizes of the droplets were consistent with the SLS results. At  $\phi_w = 0.5$  and  $[\text{E-O}/12]/[\text{MMT}] = 0.15$ , an O/W emulsion with spherical droplets of  $50 \mu\text{m}$  was formed (Figure 10a). Elongated O/W droplets were observed at  $\phi_w = 0.5$  and  $[\text{E-O}/12]/[\text{MMT}] = 0.25$  (Figure 10b). Nonspherical O/W droplets stabilized with surfactant-modified solid particles have been previously reported.<sup>27,68</sup> The W/O droplet size was about  $10 \mu\text{m}$  at  $\phi_w = 0.5$  and  $[\text{E-O}/12]/[\text{MMT}] = 0.4$  (Figure 10c) and about  $80 \mu\text{m}$  at  $\phi_w = 0.2$  and  $[\text{E-O}/12]/[\text{MMT}] = 0.25$  (Figure 10d). w/O/W emulsions were observed at  $\phi_w = 0.8$  and  $[\text{E-O}/12]/[\text{MMT}] = 0.25$  (Figure 10e). The dominant aqueous phase volume determined the outer continuous phase to be water while the mass ratio of surfactant-to-clay was high enough to form W/O droplets to be embedded in large water drops.

This clay/surfactant dispersant system demonstrates remarkable tunability and flexibility for obtaining various emulsion properties in terms of droplet size, emulsion stability, and droplet morphology by varying formulation and composition variables. In addition, understanding the influence of the transitional and catastrophic phase inversions on the associated emulsions properties would facilitate the design and development of novel dispersants for dispersing oil in seawater where the dispersant is expected to be introduced from the oil phase, but then favors the aqueous side of the interface upon emulsification.

#### 4. CONCLUSIONS

For dodecane-in-SSW emulsions formed with various concentrations of MMT clay (0.1–1% w/v) and E-O/12 surfactant (0.001–0.1% w/v) at a water volume fraction of 0.5, coalescence of oil droplets was negligible and the primary emulsion destabilization mechanism was creaming. The clay particles alone were too hydrophilic and the surfactant too hydrophobic to form these emulsions, yet the combination was highly synergistic to form oil droplets as small as  $60 \mu\text{m}$ . Thus, the surfactant interacted with the clay particles and increased the contact angle (decreased HLB of the clay) at the oil–water interface. Even when slightly lowering the HLB of MMT clay particles with only 0.001% w/v surfactant, oil-in-SSW emulsions were still formed. The pronounced synergistic effect of emulsion formation and stabilization in SSW are due in part to reduced electrostatic repulsion between adsorbed clay particles and an increase in the continuous phase viscosity.

This surfactant/clay system enabled phase inversion from W/O to O/W emulsions either by decreasing the mass ratio of surfactant-to-clay  $[\text{E-O}/12]/[\text{MMT}]$  (transitional inversion) or by increasing water volume fraction  $\phi_w$  (catastrophic inversion). For both types of emulsions, coalescence was

minimal at all conditions reported, and destabilization resulted primarily from gravity induced phase separation, which was strongly correlated with the droplet size. For intermediate values of  $\phi_w$ , increasing the  $[\text{E-O}/12]/[\text{MMT}]$  ratio inverted the curvature to a W/O emulsion, where the droplet sizes were the smallest resulting in the highest stabilities. For catastrophic inversions, the droplet size of the emulsions was smaller in the case of the preferred curvature. At high  $\phi_w$ , the creaming was faster given the more dilute oil droplets and reduction in interdroplet hydrodynamic interactions. Stable dispersions of concentrated clay in oil were obtained at high clay concentrations, which is of interest for storage stability in practical applications. The initially concentrated dispersions were diluted and sheared in seawater, whereby the mass transfer pathways crossed the catastrophic boundary resulting in  $60 \mu\text{m}$  oil droplets. The ability to mimic actual processes with these mass transfer pathways on the droplet size and stability formulation-composition diagrams will be useful for designing dispersant systems for various applications including remediating oil spills with waves and in subsea jets.

#### ■ ASSOCIATED CONTENT

##### Supporting Information

Potentiometric titration of surfactant; procedure for viscosity measurements; time dependent droplet size distribution for dodecane-in-SSW emulsions prepared with various concentrations of MMT and E-O/12; comparison of experimental creaming stability of dodecane-in-SSW emulsions with the predictions from the Stokes' law and the Richardson–Zaki model; time-dependent droplet size distribution for various  $[\text{E-O}/12]/[\text{MMT}]$  ratios and water volume fractions; droplet sizes and stabilities of emulsions prepared with various surfactant-to-clay mass ratios and water volume fractions at a total clay and surfactant concentration of 1.1% w/v. This material is available free of charge via the Internet at <http://pubs.acs.org>.

#### ■ AUTHOR INFORMATION

##### Corresponding Author

\*E-mail: [kpj@che.utexas.edu](mailto:kpj@che.utexas.edu).

##### Notes

The authors declare no competing financial interest.

#### ■ ACKNOWLEDGMENTS

This work was supported in part by the Gulf of Mexico Research Initiative and the DOE Center for Frontiers of Subsurface Energy Security. K.P.J. and T.M.T. also acknowledge the Robert A. Welch Foundation (F-1319 and F-1696, respectively). The authors thank Zheng Xue for TEM imaging, Will Hardin for BET surface analysis, and Amro Elhag for titration experiments.

#### ■ REFERENCES

- (1) Lee, K. Oil–Particle Interactions in Aquatic Environments: Influence on the Transport, Fate, Effect and Remediation of Oil Spills. *Spill Sci. Technol. Bull.* **2002**, *8* (1), 3–8.
- (2) Stoffyn-Egli, P.; Lee, K. Formation and Characterization of Oil–Mineral Aggregates. *Spill Sci. Technol. Bull.* **2002**, *8* (1), 31–44.
- (3) Zhang, H. P.; Khatibi, M.; Zheng, Y.; Lee, K.; Li, Z. K.; Mullin, J. V. Investigation of OMA Formation and the Effect of Minerals. *Mar. Pollut. Bull.* **2010**, *60* (9), 1433–1441.
- (4) Niu, H. B.; Lee, K. Study of the Dispersion/Settling of Oil–Mineral-Aggregates using Particle Tracking Model and Assessment of Their Potential Risks. *Int. J. Environ. Pollut.* **2013**, *52* (1–2), 32–51.

- (5) Binks, B. P. Particles as Surfactants—Similarities and Differences. *Curr. Opin. Colloid Interface Sci.* **2002**, *7* (1–2), 21–41.
- (6) Hunter, T. N.; Pugh, R. J.; Franks, G. V.; Jameson, G. J. The Role of Particles in Stabilising Foams and Emulsions. *Adv. Colloid Interface Sci.* **2008**, *137* (2), 57–81.
- (7) Aveyard, R.; Binks, B. P.; Clint, J. H. Emulsions Stabilised Solely by Colloidal Particles. *Adv. Colloid Interface Sci.* **2003**, *100*, 503–546.
- (8) Binks, B. P.; Rodrigues, J. A.; Frith, W. J. Synergistic Interaction in Emulsions Stabilized by a Mixture of Silica Nanoparticles and Cationic Surfactant. *Langmuir* **2007**, *23* (7), 3626–3636.
- (9) Binks, B. P.; Whitby, C. P. Nanoparticle Silica-Stabilised Oil-in-Water Emulsions: Improving Emulsion Stability. *Colloid Surf., A* **2005**, *253* (1–3), 105–115.
- (10) Binks, B. P.; Whitby, C. P. Silica Particle-Stabilized Emulsions of Silicone Oil and Water: Aspects of Emulsification. *Langmuir* **2004**, *20* (4), 1130–1137.
- (11) Binks, B. P.; Lumsdon, S. O. Stability of Oil-in-Water Emulsions Stabilised by Silica Particles. *Phys. Chem. Chem. Phys.* **1999**, *1* (12), 3007–3016.
- (12) Worthen, A. J.; Foster, L. M.; Dong, J.; Bollinger, J. A.; Peterman, A. H.; Pastora, L. E.; Bryant, S. L.; Truskett, T. M.; Bielawski, C. W.; Johnston, K. P. Synergistic Formation and Stabilization of Oil-in-Water Emulsions by a Weakly Interacting Mixture of Zwitterionic Surfactant and Silica Nanoparticles. *Langmuir* **2014**, *30* (4), 984–994.
- (13) Venkataraman, P.; Sunkara, B. S.; Dennis, J. E.; He, J. B.; John, V. T.; Bose, A. Water-in-Trichloroethylene Emulsions Stabilized by Uniform Carbon Microspheres. *Langmuir* **2012**, *28* (2), 1058–1063.
- (14) Saha, A.; Nikova, A.; Venkataraman, P.; John, V. T.; Bose, A. Oil Emulsification Using Surface-Tunable Carbon Black Particles. *ACS Appl. Mater. Interfaces* **2013**, *5* (8), 3094–3100.
- (15) Katepalli, H.; John, V. T.; Bose, A. The Response of Carbon Black Stabilized Oil-in-Water Emulsions to the Addition of Surfactant Solutions. *Langmuir* **2013**, *29* (23), 6790–6797.
- (16) Lan, Q.; Liu, C.; Yang, F.; Liu, S. Y.; Xu, J.; Sun, D. J. Synthesis of Bilayer Oleic Acid-Coated Fe<sub>3</sub>O<sub>4</sub> Nanoparticles and Their Application in pH-Responsive Pickering Emulsions. *J. Colloid Interface Sci.* **2007**, *310* (1), 260–269.
- (17) Ingram, D. R.; Kotsmar, C.; Yoon, K. Y.; Shao, S.; Huh, C.; Bryant, S. L.; Milner, T. E.; Johnston, K. P. Superparamagnetic Nanoclusters Coated with Oleic Acid Bilayers for Stabilization of Emulsions of Water and Oil at Low Concentration. *J. Colloid Interface Sci.* **2010**, *351* (1), 225–232.
- (18) Zhou, J.; Qiao, X. Y.; Binks, B. P.; Sun, K.; Bai, M. W.; Li, Y. L.; Liu, Y. Magnetic Pickering Emulsions Stabilized by Fe<sub>3</sub>O<sub>4</sub> Nanoparticles. *Langmuir* **2011**, *27* (7), 3308–3316.
- (19) Yoon, K. Y.; Li, Z.; Neilson, B. M.; Lee, W.; Huh, C.; Bryant, S. L.; Bielawski, C. W.; Johnston, K. P. Effect of Adsorbed Amphiphilic Copolymers on the Interfacial Activity of Superparamagnetic Nanoclusters and the Emulsification of Oil in Water. *Macromolecules* **2012**, *45* (12), 5157–5166.
- (20) Lagaly, G.; Ziesmer, S. Colloid Chemistry of Clay Minerals: the Coagulation of Montmorillonite Dispersions. *Adv. Colloid Interface Sci.* **2003**, *100*, 105–128.
- (21) Mejia, A. F.; Diaz, A.; Pulella, S.; Chang, Y. W.; Simonetty, M.; Carpenter, C.; Batteas, J. D.; Mannan, M. S.; Clearfield, A.; Cheng, Z. D. Pickering Emulsions Stabilized by Amphiphilic Nano-Sheets. *Soft Matter* **2012**, *8* (40), 10245–10253.
- (22) Lagaly, G.; Reese, M.; Abend, S. Smectites as Colloidal Stabilizers of Emulsions—I. Preparation and Properties of Emulsions with Smectites and Nonionic Surfactants. *Appl. Clay Sci.* **1999**, *14* (1–3), 83–103.
- (23) Luckham, P. F.; Rossi, S. The Colloidal and Rheological Properties of Bentonite Suspensions. *Adv. Colloid Interface Sci.* **1999**, *82* (1–3), 43–92.
- (24) Leach, E. S. H.; Hopkinson, A.; Franklin, K.; van Duijneveldt, J. S. Nonaqueous Suspensions of Laponite and Montmorillonite. *Langmuir* **2005**, *21* (9), 3821–3830.
- (25) Segad, M.; Jonsson, B.; Cabane, B. Tactoid Formation in Montmorillonite. *J. Phys. Chem. C* **2012**, *116* (48), 25425–25433.
- (26) Torres, L. G.; Iturbe, R.; Snowden, M. J.; Chowdhry, B. Z.; Leharne, S. A. Preparation of O/W Emulsions Stabilized by Solid Particles and Their Characterization by Oscillatory Rheology. *Colloid Surf., A* **2007**, *302* (1–3), 439–448.
- (27) Zhang, J.; Li, L.; Xu, J.; Sun, D. Effect of Cetyltrimethylammonium Bromide Addition on the Emulsions Stabilized by Montmorillonite. *Colloid Polym. Sci.* **2014**, *292* (2), 441–447.
- (28) Cui, Y. N.; van Duijneveldt, J. S. Microcapsules Composed of Cross-Linked Organoclay. *Langmuir* **2012**, *28* (3), 1753–1757.
- (29) Cui, Y. N.; Threlfall, M.; van Duijneveldt, J. S. Optimizing Organoclay Stabilized Pickering Emulsions. *J. Colloid Interface Sci.* **2011**, *356* (2), 665–671.
- (30) Gelot, A.; Friesen, W.; Hamza, H. A. Emulsification of Oil and Water in the Presence of Finely Divided Solids and Surface-Active Agents. *Colloids Surf.* **1984**, *12* (3–4), 271–303.
- (31) Sekine, T.; Yoshida, K.; Matsuzaki, F.; Yanaki, T.; Yamaguchi, M.; Novel, A. Method for Preparing Oil-in-Water-in-Oil Type Multiple Emulsions Using Organophilic Montmorillonite Clay Mineral. *J. Surfactants Deterg.* **1999**, *2* (3), 309–315.
- (32) Binks, B. P.; Clint, J. H.; Whitby, C. P. Rheological Behavior of Water-in-Oil Emulsions Stabilized by Hydrophobic Bentonite Particles. *Langmuir* **2005**, *21* (12), 5307–5316.
- (33) Whitby, C. P.; Fornasiero, D.; Ralston, J. Effect of Oil Soluble Surfactant in Emulsions Stabilised by Clay Particles. *J. Colloid Interface Sci.* **2008**, *323* (2), 410–419.
- (34) Wang, J.; Liu, G. P.; Wang, L. Y.; Li, C. F.; Xu, J. A.; Sun, D. J. Synergistic Stabilization of Emulsions by Poly(oxypropylene)Diamine and Laponite Particles. *Colloids Surf., A* **2010**, *353* (2–3), 117–124.
- (35) Li, W.; Yu, L. J.; Liu, G. P.; Tan, J. J.; Liu, S. Y.; Sun, D. J. Oil-in-Water Emulsions Stabilized by Laponite Particles Modified with Short-Chain Aliphatic Amines. *Colloids Surf., A* **2012**, *400*, 44–51.
- (36) Tsugita, A.; Takemoto, S.; Mori, K.; Yoneya, T.; Otani, Y. Studies on O/W Emulsions Stabilized with Insoluble Montmorillonite–Organic Complexes. *J. Colloid Interface Sci.* **1983**, *95* (2), 551–560.
- (37) Wang, J.; Yang, F.; Tan, J. J.; Liu, G. P.; Xu, J.; Sun, D. J. Pickering Emulsions Stabilized by a Lipophilic Surfactant and Hydrophilic Platelike Particles. *Langmuir* **2010**, *26* (8), 5397–5404.
- (38) Paunov, V. N.; Binks, B. P.; Ashby, N. P. Adsorption of Charged Colloid Particles to Charged Liquid Surfaces. *Langmuir* **2002**, *18* (18), 6946–6955.
- (39) Golemanov, K.; Tcholakova, S.; Kralchevsky, P. A.; Ananthapadmanabhan, K. P.; Lips, A. Latex-Particle-Stabilized Emulsions of Anti-Bancroft Type. *Langmuir* **2006**, *22* (11), 4968–4977.
- (40) Tcholakova, S.; Denkov, N. D.; Lips, A. Comparison of Solid Particles, Globular Proteins and Surfactants as Emulsifiers. *Phys. Chem. Chem. Phys.* **2008**, *10* (12), 1608–1627.
- (41) Ashby, N. P.; Binks, B. P. Pickering Emulsions Stabilised by Laponite Clay Particles. *Phys. Chem. Chem. Phys.* **2000**, *2* (24), 5640–5646.
- (42) Salager, J. L.; Marquez, L.; Pena, A. A.; Rondon, M.; Silva, F.; Tyrode, E. Current Phenomenological Know-How and Modeling of Emulsion Inversion. *Ind. Eng. Chem. Res.* **2000**, *39* (8), 2665–2676.
- (43) Salager, J. L.; Forgiarini, A.; Marquez, L.; Pena, A.; Pizzino, A.; Rodriguez, M. P.; Rondo-Gonzalez, M. Using Emulsion Inversion in Industrial Processes. *Adv. Colloid Interface Sci.* **2004**, *108*, 259–272.
- (44) Salager, J. L.; Forgiarini, A. M. Emulsion Stabilization, Breaking, and Inversion Depends upon Formulation: Advantage or Inconvenience in Fow Assurance. *Energy Fuels* **2012**, *26* (7), 4027–4033.
- (45) Bancroft, W. D. The Theory of Emulsification. *V. J. Phys. Chem.* **1913**, *17* (6), 501–519.
- (46) Binks, B. P.; Lumsdon, S. O. Catastrophic Phase Inversion of Water-in-Oil Emulsions Stabilized by Hydrophobic Silica. *Langmuir* **2000**, *16* (6), 2539–2547.



- (47) Binks, B. P.; Lumsdon, S. O. Transitional Phase Inversion of Solid-Stabilized Emulsions Using Particle Mixtures. *Langmuir* **2000**, *16* (8), 3748–3756.
- (48) Binks, B. P.; Lumsdon, S. O. Influence of Particle Wettability on the Type and Stability of Surfactant-Free Emulsions. *Langmuir* **2000**, *16* (23), 8622–8631.
- (49) Stiller, S.; Gers-Barlag, H.; Lergenmueller, M.; Pflucker, F.; Schulz, J.; Wittern, K. P.; Daniels, R. Investigation of the Stability in Emulsions Stabilized with Different Surface Modified Titanium Dioxides. *Colloids Surf, A* **2004**, *232* (2–3), 261–267.
- (50) Binks, B. P.; Lumsdon, S. O. Pickering Emulsions Stabilized by Monodisperse Latex Particles: Effects of Particle Size. *Langmuir* **2001**, *17* (15), 4540–4547.
- (51) Zhang, J. C.; Li, L.; Wang, J.; Sun, H. G.; Xu, J.; Sun, D. J. Double Inversion of Emulsions Induced by Salt Concentration. *Langmuir* **2012**, *28* (17), 6769–6775.
- (52) Zhang, J. C.; Li, L.; Wang, J.; Xu, J.; Sun, D. J. Phase Inversion of Emulsions Containing a Lipophilic Surfactant Induced by Clay Concentration. *Langmuir* **2013**, *29* (12), 3889–3894.
- (53) Wang, J.; Yang, F.; Li, C. F.; Liu, S. Y.; Sun, D. J. Double Phase Inversion of Emulsions Containing Layered Double Hydroxide Particles Induced by Adsorption of Sodium Dodecyl Sulfate. *Langmuir* **2008**, *24* (18), 10054–10061.
- (54) Cui, Z. G.; Cui, C. F.; Zhu, Y.; Binks, B. P. Multiple Phase Inversion of Emulsions Stabilized by in Situ Surface Activation of CaCO<sub>3</sub> Nanoparticles via Adsorption of Fatty Acids. *Langmuir* **2012**, *28* (1), 314–320.
- (55) Binks, B. P.; Rodrigues, J. A. Double Inversion of Emulsions by Using Nanoparticles and a Di-Chain Surfactant. *Angew. Chem., Int. Ed.* **2007**, *46* (28), 5389–5392.
- (56) Binks, B. P.; Rodrigues, B. A. Influence of Surfactant Structure on the Double Inversion of Emulsions in the Presence of Nanoparticles. *Colloids Surf, A* **2009**, *345* (1–3), 195–201.
- (57) Binks, B. P.; Desforges, A.; Duff, D. G. Synergistic Stabilization of Emulsions by a Mixture of Surface-Active Nanoparticles and Surfactant. *Langmuir* **2007**, *23* (3), 1098–1106.
- (58) Connolly, J.; van Duijneveldt, J. S.; Klein, S.; Pizzey, C.; Richardson, R. M. Effect of Surfactant and Solvent Properties on the Stacking Behavior of Non-Aqueous Suspensions of Organically Modified Clays. *Langmuir* **2006**, *22* (15), 6531–6538.
- (59) James, A. D.; Wates, J. M.; Wyn-Jones, E. Determination of the Hydrophilicities of Nitrogen-Based Surfactants by Measurement of Partition-Coefficients between Heptane and Water. *J. Colloid Interface Sci.* **1993**, *160* (1), 158–165.
- (60) Richardson, J. F.; Zaki, W. N. The Sedimentation of a Suspension of Uniform Spheres under Conditions of Viscous Flow. *Chem. Eng. Sci.* **1954**, *3* (2), 65–73.
- (61) Mohan, S.; Narsimhan, G. Coalescence of Protein-Stabilized Emulsions in a High-Pressure Homogenizer. *J. Colloid Interface Sci.* **1997**, *192* (1), 1–15.
- (62) Marinova, K. G.; Alargova, R. G.; Denkov, N. D.; Velev, O. D.; Petsev, D. N.; Ivanov, I. B.; Borwankar, R. P. Charging of Oil–Water Interfaces due to Spontaneous Adsorption of Hydroxyl Ions. *Langmuir* **1996**, *12* (8), 2045–2051.
- (63) Denkov, N. D.; Ivanov, I. B.; Kralchevsky, P. A.; Wasan, D. T. A Possible Mechanism of Stabilization of Emulsions by Solid Particles. *J. Colloid Interface Sci.* **1992**, *150* (2), 589–593.
- (64) Madivala, B.; Vandebriel, S.; Franssaer, J.; Vermant, J. Exploiting Particle Shape in Solid Stabilized Emulsions. *Soft Matter* **2009**, *5* (8), 1717–1727.
- (65) Salager, J. L.; Loaiza-Maldonado, I.; Minana-Perez, M.; Silva, F. Surfactant-Oil-Water Systems Near the Affinity Inversion. I. Relationship between Equilibrium Phase-Behavior and Emulsion Type and Stability. *J. Dispersion Sci. Technol.* **1982**, *3* (3), 279–292.
- (66) Langevin, D. Influence of Interfacial Rheology on Foam and Emulsion Properties. *Adv. Colloid Interface Sci.* **2000**, *88* (1–2), 209–222.
- (67) Kaptay, G. On the Equation of the Maximum Capillary Pressure Induced by Solid Particles to Stabilize Emulsions and Foams and on the Emulsion Stability Diagrams. *Colloids Surf, A* **2006**, *282*, 387–401.
- (68) Ravera, F.; Ferrari, M.; Liggieri, L.; Loglio, G.; Santini, E.; Zanobini, A. Liquid–Liquid Interfacial Properties of Mixed Nanoparticle–Surfactant Systems. *Colloids Surf, A* **2008**, *323* (1–3), 99–108.